PNAS
www.pnas.org

Supplementary Information for

Cooperation mitigates diversity loss in a spatially expanding microbial population

Saurabh R. Gandhi[1], Kirill S. Korolev*[2,3], Jeff Gore*[1]

Jeff Gore

Email: gore@mit.edu

Kirill Korolev

Email: korolev@bu.edu

This PDF file includes:

Supplementary text

Figures S1 to S5

Tables S1

Supplementary Information

Simulations

The simulations corresponding to Fig. 4 in the main text, showing differences in the dynamics during selective sweeps and jackpots were set up to closely follow the experiments. The two cell subpopulations (for instance, corresponding to RFP and YFP) start at equal fractions, with an exponential profile in space. For every cycle, the densities of all subpopulations at the end of the cycle are computed based on deterministic logistic growth, where the carrying capacity of the total population is held fixed. The number of cells transferred to the front and back are drawn from a Poisson distribution with mean given by $\langle n_{x\pm1}\rangle = n_x(\frac{m}{2})/df$, where m is the migration rate and df is the dilution factor. The Poisson sampling in migration is the source of stochasticity that results in the occasional jackpots.

For the selective sweep case, we repeat the simulations as above, but with 4 instead of 2 subpopulations, corresponding to WT and mutant types of both initial strains. The mutant subpopulations start with 0 density. For each cycle, a small fraction of the final WT cells can become mutants with a higher growth rate. The final number of mutants is also determined by binomial sampling from the WT numbers with a very small probability.

All subsequent analysis is identical to what is done with experimental data.

Estimation of low density growth rates

Low density growth rates of the two strains of yeast in different media were measured by directly by measuring initial and final densities at the end of 4 hours in conditions similar to the ones for the expansion experiments (no shaking, same temperature, humidity and media volumes). The yeast start with a wide range of initial densities, with a 1:1 ratio of the two fluorescent genotypes, and undergo 4-5 cycles of growth and dilution, to remove transient effects. The initial and final densities are measured for one cycle after that. The densities are measured by diluting the cultures (1x or no dilution if wells look clear, higher dilution rates such as 5x as required if wells are visually cloudy) in PBS, and then directly counting cells on a MACS flow cytometer. Appropriate gates were applied on the forward scatter, side scatter and fluorescent channels to remove noise. The data is shown in SI Fig. 1, and we describe the analysis procedure below.

For each media/strain, we apply a moving window across the entire range of measured initial densities, and calculate the mean growth rate in each window. We computed such a moving average growth rate for all media/strain combinations for 4 different window sizes: 20%, 30%, 40% and 50% of the entire range of initial densities.

We find that for all window sizes, the mean growth rates at the lowest initial densities are nearly equal, and certainly within 1 SEM of one-another, indicating that the exact window size chosen for the growth rate estimation does not affect the estimate significantly compared to the measurement uncertainty itself (SI Fig. 2). However, the smallest window size has very few, noisy data points, whereas larger window sizes average over a broader range of initial densities and get affected by growth rates at higher densities. Thus, we use the mean and SEM from the 30% window at the lowest initial density range to compute the Fisher velocities and their uncertainties. SI Fig. 1 shows results for a window size of 30%.

As can be seen in SI Fig. 1, both strains DH and BY grow without any Allee effect in galactose (1st column on the left). For DH growing on glucose, the growth rate at low densities can be seen to be the same (0.43

/hr) in 0.2% and 0.02% glucose. However, at intermediate densities, growth rate in 0.2% glucose increases significantly above the low-density value (causing an Allee effect, and slightly pushed waves), unlike in 0.02% glucose (where growth rate remains equal to or less than the low-density estimate). This suggests that while the strains can generally grow at a faster rate in higher concentrations of glucose, at low densities, the growth rate is limited by something other than glucose, and thus, is not modulated by glucose concentrations. Both strains, DH and BY show a clear Allee effect when growing on sucrose (SI Fig. 1 red panels).

SI Fig. 1: Density dependence of growth rate and fits for low density growth rate for different strain-media combinations.

Each panel shows the growth profile of the indicated yeast strain on a specific growth medium. Each point in a panel represents a measurement of the mean growth rate ($r = 1/T\ ln(N_f/N_i)$) in a single well starting at the given initial density. A sliding window (with size equal to 30% of the entire initial density range) is applied over the range of initial densities. Errorbars show the location where a window is centered, and the size of the errorbar gives the SEM of the estimated growth rate within that window. The shaded grey region is the lowest window, which was used for the low-density growth rate estimation. The shaded colored region is the growth rate range for the lowest density, shown as an aid to visualize the Allee effect.

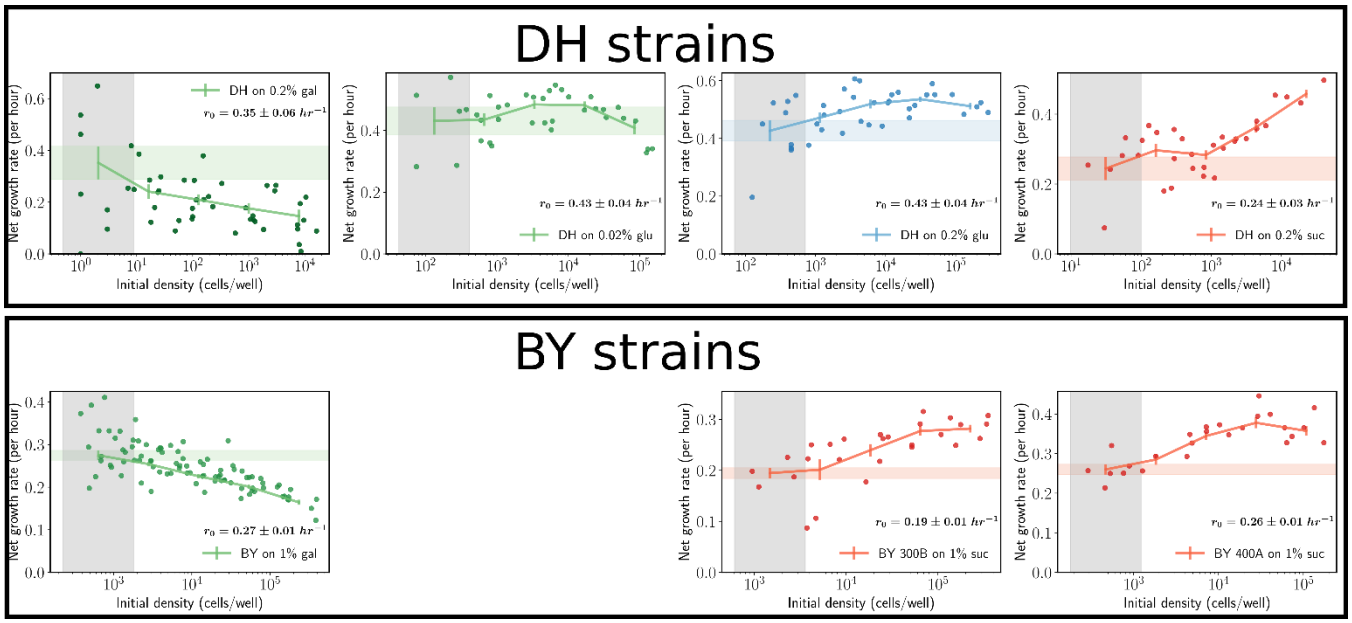

SI Fig. 2: Estimates of low density growth rates are not affected by choice of window size

Low density growth rates were estimated by sliding a window across the range of initial densities, and computing the average growth rate in each window. The window size is set as a fixed fraction of the total initial density range. The mean growth rate for all window sizes is within the SEM, indicating that the choice of window size does not significantly change the growth rate, and thus Fisher velocity estimates.

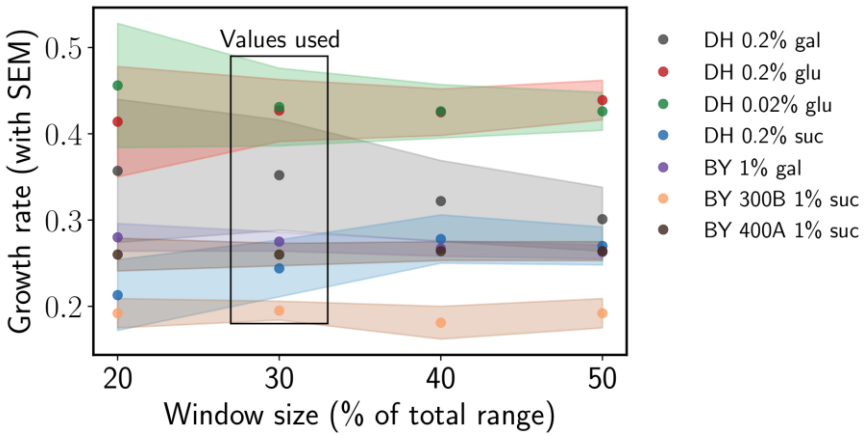

SI Fig. 3: Jackpots in experiments. Jackpots are rare events where stochasticity in migration leads to the front elongating at the very tip, leading to rapid change of fractions of the genotypes. The figure shows 4 instances of jackpots in our experiments. Left panel shows the trajectory of the experiment in the front width-velocity state space, where the axes are rescaled so that both the front width and the velocity have mean 0 and std. dev. 1. For jackpots, such trajectories transiently move to (or start from) the top right but eventually move back towards the mean (transient elongation of the front accompanied by increased velocity). The right panels show the specific replicate that underwent a jackpot event, compared to the rest of the replicates in the same experiment. For one experiment (DH expanding in 0.2% suc, top panel), we suspect a few cells at the front were transferred more than one wells, likely due to a droplet blowing across while pipetting. This was reflected in a small new wavefront emerging ahead of the original front. The two fronts eventually merged in a manner similar to the embolism effect described in the main text. This extreme event resulted in a jackpot even though the expansion is pushed.

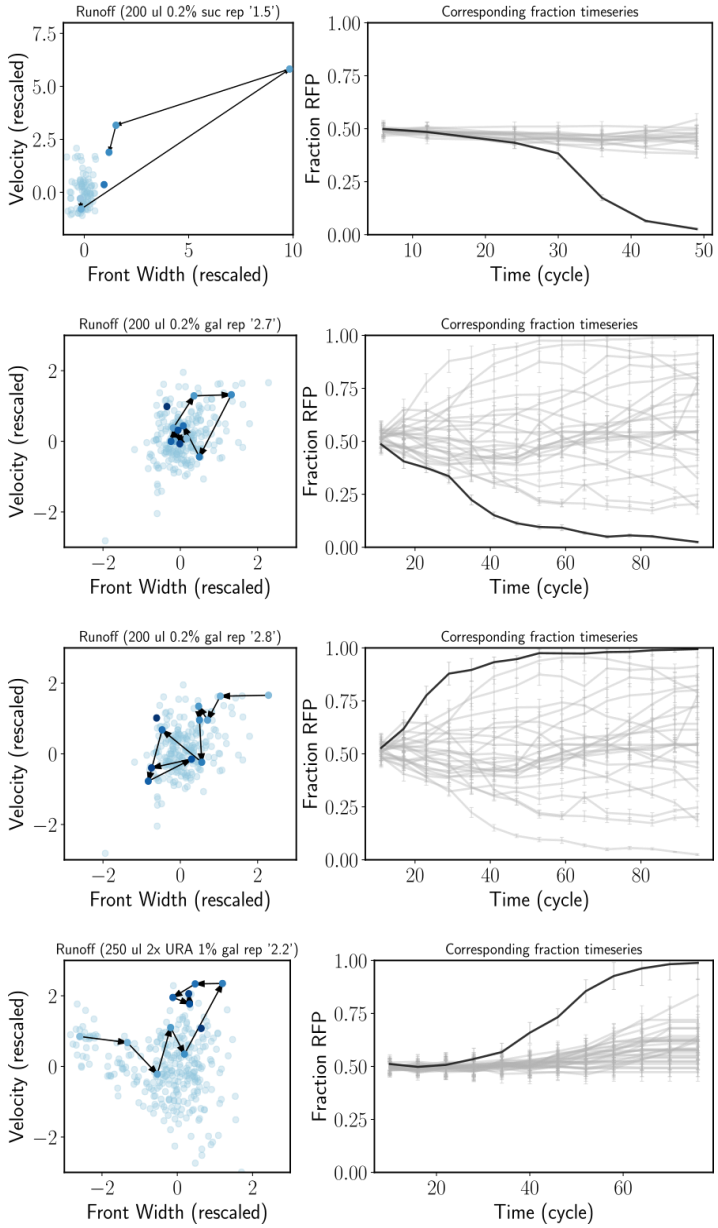

SI Fig. 4: All evolution state space diagrams. Similar to jackpot events, when a faster growing mutant appears in the front, the mutant fraction again increases quickly. However, in contrast to jackpots, where the state space trajectories relax back to equilibrium values, for selective sweeps, the front width decreases and the velocity increases permanently, leading to trajectories that move to the top left in the state space diagram and stay there. The figure shows 6 instances of selective sweeps observed in our experiments.

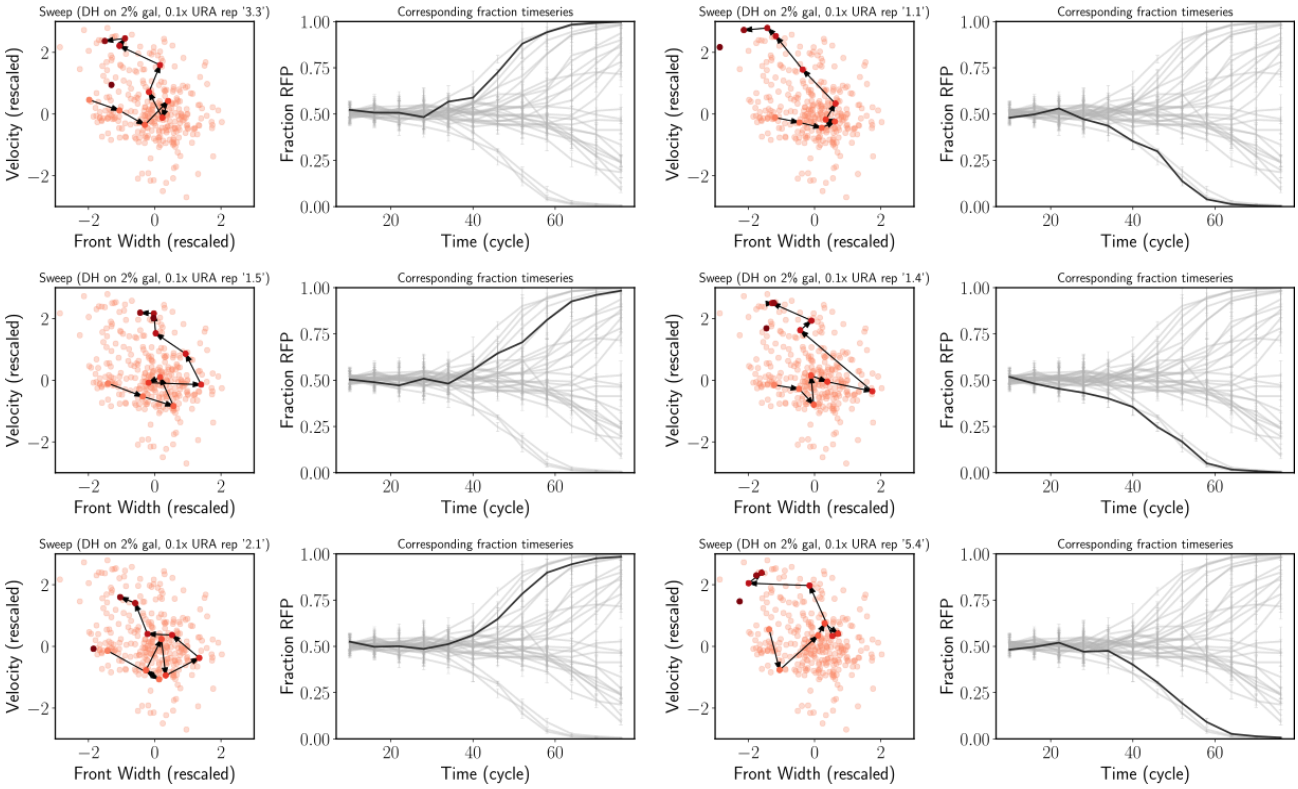

SI Fig. 5: Front diffusion in pulled and pushed expansions. The expansion wavefront is known to diffuse around its mean position as the population expands. The diffusion coefficient is determined by the intrinsic demographic stochasticity in the population as well as the environmental noise. Pulled waves are predicted to be dominated by intrinsic stochasticity, and typically diffuse more around the mean compared to pushed waves, where front diffusion is predicted to be dominated by environmental noise. However, in our experiments, we did not find a significant difference in pulled and pushed waves, suggesting that the diffusion of the front is dominated by environmental noise in both cases, induced by the sampling noise in migration and dilution.

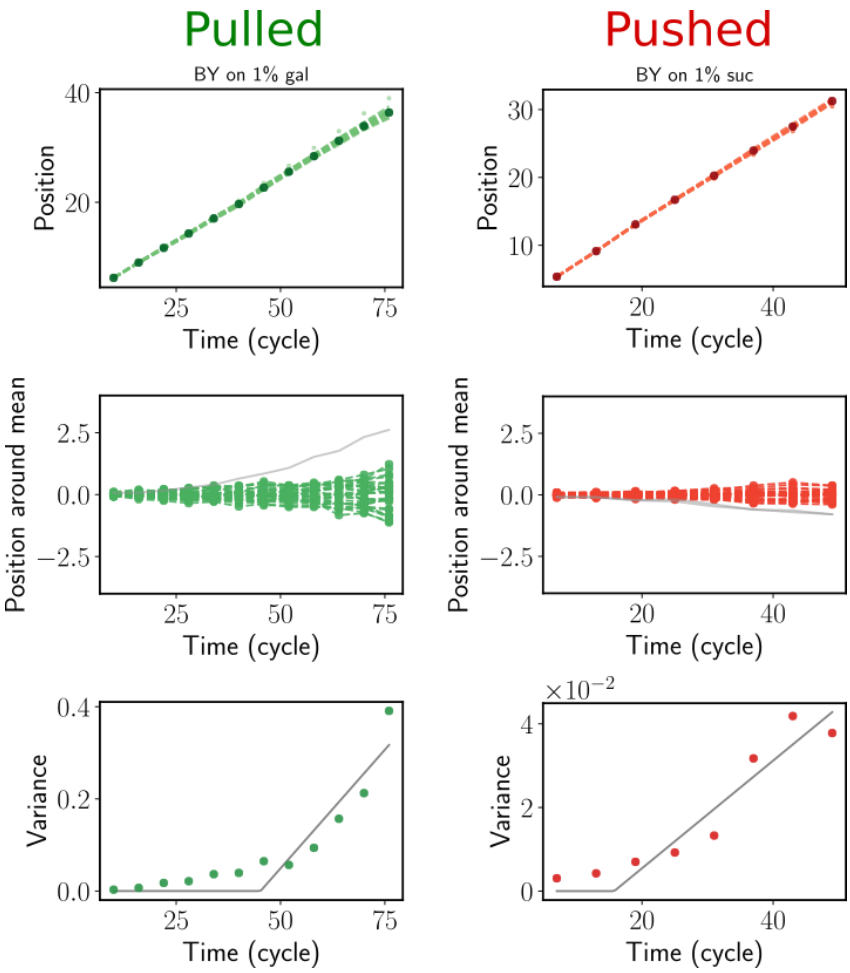

SI Table 1: Details of experimental parameters for data shown in Fig. 3C, D

#	Strain, Media	Migration Rate	Dilution Factor	# Replicates	# Cycles
1	BY, 250 ul 2x URA + 1% suc	0.3	2	30	59
2	BY, 250 ul 2x URA + 1% suc	0.3	2	30	59
3	DH, 200 ul 0.2% suc	0.3	2	16	50
4	DH, 200 ul 0.2% glu	0.3	2	16	50
5	DH, 200 ul 0.2% glu	0.3	2	40	82
6	DH, 200 ul 0.2% glu	0.5	2	40	65
7	DH, 200 ul 0.4% glu	0.3	2	16	48
8	DH, 200 ul 0.4% glu	0.25	1.54	8	48
9	DH, 200 ul 0.4% glu	0.25	1.33	8	48
10	BY, 250 ul 2x URA + 1% gal	0.3	2	30	74
11	DH, 200 ul 0.2% gal	0.4	2	24	102
12	DH, 200 ul 0.02% glu	0.4	2	16	40
13	DH, 200 ul 0.01% glu	0.4	2	36	73

As the table indicates, a few experimental conditions (media/strain pair, migration and dilution rates) were repeated in order to test the robustness of results. Data from such experiments is analyzed independently instead of pooling, because a number of small factors vary a little bit across experiments, such as the batch of media, the starting yeast cultures, the starting ratios of the two genotypes etc. Given these differences, with the last one being particularly important (the exact ratio of genotypes in the starting culture), statistical artifacts could be introduced if data from different experiments is pooled together. Moreover, in most cases, the number of cycles for which the experiment is performed also changes, and pooling would require discarding all data beyond the minimum common number of cycles.